Journal of Dental Research
2016, Vol. 95(3) 319–326

DOI: 10.1177/0022034515616760
jdr.sagepub.com

Topography Influences Adherent Cell Regulation of Osteoclastogenesis

M. Nagasawa[1,2], L.F. Cooper[1], Y. Ogino[3], D. Mendonca[4], R. Liang[1], S. Yang[5], G. Mendonca[4], and K. Uoshima[2]

Abstract

The importance of osteoclast-mediated bone resorption in the process of osseointegration has not been widely considered. In this study, cell culture was used to investigate the hypothesis that the function of implant-adherent bone marrow stromal cells (BMSCs) in osteoclastogenesis is influenced by surface topography. BMSCs isolated from femur and tibia of Sprague-Dawley rats were seeded onto 3 types of titanium surfaces (smooth, micro, and nano) and a control surface (tissue culture plastic) with or without osteogenic supplements. After 3 to 14 d, conditioned medium (CM) was collected. Subsequently, rat bone marrow–derived macrophages (BMMs) were cultured in media supplemented with soluble receptor activator of NF-κB ligand (RANKL) and macrophage colony-stimulating factor (M-CSF) as well as BMSC CM from each of the 4 surfaces. Gene expression levels of soluble RANKL, osteoprotegerin, tumor necrosis factor α, and M-CSF in cultured BMSCs at different time points were measured by real-time polymerase chain reaction. The number of differentiated osteoclastic cells was determined after tartrate-resistant acid phosphatase staining. Analysis of variance and *t* test were used for statistical analysis. The expression of prominent osteoclast-promoting factors tumor necrosis factor α and M-CSF was increased by BMSCs cultured on both micro- and nanoscale titanium topographies ($P < 0.01$). BMSC CM contained a heat-labile factor that increased BMMs osteoclastogenesis. CM from both micro- and nanoscale surface-adherent BMSCs increased the osteoclast number ($P < 0.01$). Difference in surface topography altered BMSC phenotype and influenced BMM osteoclastogenesis. Local signaling by implant-adherent cells at the implant-bone interface may indirectly control osteoclastogenesis and bone accrual around endosseous implants.

Keywords: biomaterial, dental implant, osteoblast, osteoclast, osseointegration, tissue engineering

Introduction

The concept of osseointegration is widely accepted in clinical implantology. However, difficult clinical scenarios challenge success (Klokkevold and Han 2007). Technological efforts that favor the rapid establishment of osseointegration enable rapid bone accrual (Ogle 2015). Implant surface topography is a key factor that influences osseointegration by enhancing surface-adherent osteoprogenitor cell differentiation and bone matrix formation (Dalby et al. 2007). However, bone mass is known to represent the balance between bone formation by osteoblasts and bone resorption activities of osteoclasts. The importance of osteoclast-mediated bone resorption in the process of osseointegration has not been widely considered. The osteoclast may resorb adjacent bone as well as interact with the implant surface during initial healing and is involved in the remodeling of interfacial bone throughout the functioning lifetime of the implant (Minkin and Marinho 1999).

Osteoclastogenesis is coupled with osteoblast function; it is affected most directly by the differentiating osteoblast expression of receptor activator of NF-κB ligand (RANKL) and osteoprotegerin (OPG), which stimulates and suppresses osteoclast differentiation, respectively. Endosseous implant topography influences surface-adherent osteoprogenitor cell expression of many bone-related proteins that influence osteoclastogenesis, including OPG and RANKL (Schwartz et al. 2009). These observations have been made at many levels in vitro and in vivo (Thalji and Cooper 2013, 2014). The influence of surface topography on adherent cell function clearly extends beyond the osteoprogenitor cell type.

While proliferation and differentiation of the cells cultured directly on titanium surface have been studied widely, the indirect effects of titanium on peripheral cells are yet to be elucidated. Osteoblast-derived and osteoclast-related cytokines and

[1]Bone Biology and Implant Therapy Laboratory, School of Dentistry, University of North Carolina, Chapel Hill, NC, USA
[2]Division of Bio-prosthodontics, Niigata University Graduate School of Medical and Dental Sciences, Nigata, Japan
[3]Department of Oral Rehabilitation, Kyushu University, Fukuoka, Japan
[4]Department of Biologic and Materials Sciences, Division of Prosthodontics, School of Dentistry, University of Michigan, Ann Arbor, MI, USA
[5]College of Stomatology, Chongqing Medical University, Chongqing, China

A supplemental appendix to this article is published electronically only at http://jdr.sagepub.com/supplemental.

Corresponding Author:
L.F. Cooper, Bone Biology and Implant Therapy Laboratory, School of Dentistry, University of North Carolina, 4610 Koury Oral Health Sciences Building CB #7450, Chapel Hill, NC 27599-7260, USA.
Email: Lyndon_Cooper@unc.edu

growth factors might play important roles in the establishment of osseointegration. Thus, we hypothesized that titanium surface–adherent cells exhibit indirect influences on the process of osteoclast differentiation.

Materials and Methods

Preparation of Titanium Disks

Commercially available pure-grade IV titanium disks (20.0 × 1.0 mm) were prepared, and the surfaces were modified into 3 kinds of topography: smooth (S), micro (M), and nano (N). The sequence for disk preparation was performed as previously described (Mendonca et al. 2010; Ogino et al. 2016).

Surface Analysis

Scanning electron microscopy (SEM) analysis of the prepared disk surfaces was performed with a high-resolution field emission SEM (S-4700; Hitachi, Tokyo, Japan), atomic force microscopy (probe = WZS; JSPM-4210; JEOL, Tokyo, Japan), and x-ray photoelectron spectroscopy (Quantum-2000 Scanning ESCS Microprobe; ULVAC-PHI Inc., Tokyo, Japan). Observations were made at 3 locations on a disk surface, and 3 disks were measured. Average values and standard deviations were then calculated.

BMSC Cell Culture and Conditioned Medium Preparation

Bone marrow stromal cells (BMSCs) were isolated from 6-wk-old male Sprague-Dawley rats. Rats were sacrificed by CO_2 inhalation, and femur and tibia were removed aseptically. Bone marrow was flushed out with high-glucose Dulbecco's modified Eagle's medium (HG-DMEM; Lonza, Basel, Switzerland) with 1% penicillin and streptomycin (Invitrogen, Carlsbad, CA, USA). Cells were cultured in HG-DMEM supplemented with 10% fetal bovine serum and 1% penicillin and streptomycin in a humidified atmosphere of 95% air and 5% CO_2 at 37 °C. The cells were washed, and the nonadherent cells were removed after 24 h. At 80% confluency, cells were passaged and seeded onto the titanium disks (1×10^5 cells/disk). Osteoblastic differentiation was induced with media containing 0.2 mM ascorbic acid, 10 mM beta-glycerophosphate, and 10^{-7}M dexamethasone. After 3, 7, and 14 d, conditioned medium (CM) was collected and stored at –80 °C until use.

BMM Cell Culture

Bone marrow–derived macrophages (BMMs) were harvested from femur and tibia of 6-wk-old Sprague-Dawley rats and cultured in HG-DMEM supplemented with 10% fetal bovine serum and 1% penicillin and streptomycin in a humidified atmosphere of 95% air and 5% CO_2 at 37 °C. The nonadherent cells were collected after 24 h and used for osteoclast formation assay. The cells were seeded at a concentration of 1×10^6 cells/mL and cultured for 4 d in HG-DMEM supplemented with 20% fetal bovine serum, recombinant murine soluble RANKL (50 ng/mL; PeproTech, London, UK), macrophage colony-stimulating factor (M-CSF; 20 ng/mL; PeproTech), 1% penicillin-streptomycin, and the CM from the supernatant of BMSCs cultured on titanium discs.

Cell Proliferation Assay

The CellTiter 96 Aqueous One Solution Cell Proliferation Assay Kit (Promega, Mannheim, Germany) was used for cell quantification. BMSCs (1×10^5 cells/mL) were seeded onto the titanium disks (S, M, N). At 3, 7, and 14 d of BMSC culture on titanium disks (each sample, $n = 6$) with regular medium (RM) or osteogenic medium (OM), the cells were treated with MTS solution—3-(4,5-dimethylthiazol-2-yl)-5-(3-carboxy methoxyphenyl)-2-(4-sulfophenyl)-2H-tetrazolium—in culture medium at 37 °C under air plus 5% CO_2 for 3 h. Absorbance at 490 nm of the supernatant was measured with a microplate reader (BioTek Instrument, Bad Friedrichshall, Germany) with Gene5 software. The differentiated osteoclast numbers were adjusted according to this ratio.

Mineralization

BMSCs cultured with RM or OM on tissue culture plastic (TCP) were fixed with 4% formaldehyde after 14 and 21 d of culture, and each well was stained with 2% alizarin red (Sigma-Aldrich, St. Louis, MO, USA). Stained cultures were scanned with the ScanJet 6100C (Hewlett-Packard Inc., Palo Alto, CA, USA).

Quantitative Real-time PCR

Total RNA of BMSCs cultured on titanium disks and BMMs were extracted with TRIzol Reagent (Life Technologies, Carlsbad, CA, USA) and purified. The RNA concentrations were then determined spectrophotometrically. From each total RNA sample, cDNA was generated with SuperScript VILO Master Mix (Life Technologies). Quantitative real-time polymerase chain reactions were performed with SYBR Green PCR Master Mix (Applied Biosystems, Foster City, CA, USA) and thermocycling (Applied Biosystems 7500). The genes analyzed were runt-related transcription factor 2 (Runx2), bone sialoprotein (BSP), osterix (OSX), alkaline phosphatase (ALP), OPG, tumor necrosis factor α (TNF-α), M-CSF, and RANKL in BMSCs and tartrate-resistant acid phosphatase (TRAP) and cathepsin K in BMMs. Relative mRNA abundance was determined by the comparative Ct method and reported as fold induction. GAPDH abundance was used for normalization. We triplicated the experiment at once, and we carried out this 3 times.

Animal Surgery

All procedures were approved by the Institutional Animal Care and Use Committee, University of North Carolina at Chapel Hill. The guidelines for in vivo experiments in animals were adhered to. Commercially pure titanium implants (S, M, and N) were implanted in the tibiae of Sprague-Dawley rats, and

Table. Ion Composition Data from X-ray Photoelectron Spectroscopy Analysis.

	Atomic Concentration,[a] %					
	O1s	C1s	Ti2p	Na1s	N1s	S2p
Smooth	44.8 ± 2.4	36.2 ± 2.2	10.9 ± 0.5	4.9 ± 1.4	2.4 ± 0.4	0.8 ± 1.2
Micro	47.0 ± 2.6	29.6 ± 4.5	17.7 ± 1.5	3.1 ± 0.4	2.1 ± 0.6	0.5 ± 0.3
Nano	51.6 ± 2.5	25.4 ± 1.6	18.1 ± 1.5	2.6 ± 1.2	1.7 ± 0.6	0.5 ± 0.3

[a]Oxygen, carbon, titanium, sodium, nitrogen, and sulfur.

bone marrow was flushed out with the medium and harvested 1 d after implantation (Masuda et al. 1997; Fujii et al. 1998; Futami et al. 2000; see Appendix for details). BMMs were cultured as described previously. The samples investigated consisted of 5 tibia from 3 rats.

TRAP Staining

To identify osteoclasts, BMMs were plated in 96-well plates at a seeding density of 1×10^6 cells/mL and cultured for 4 d. At the end of culture, the cells were fixed in a mixture of citrate (6.75 mM), acetone (65%), and formalin (3.7%) for 90 s at room temperature. TRAP staining solution was prepared according to the manufacturer's recommended protocol (Sigma). Cells were incubated in the TRAP staining solution for 10 min at 37 °C, and the reaction was stopped by rinsing with tap water (Kang et al. 2010). The number of TRAP+ multinucleated (≥3 nuclei) cells, considered to be osteoclasts, was determined by microscopic counts (Takayanagi et al. 2000). All data are expressed as mean ± SEM ($n = 7$).

Enzyme-linked Immunosorbent Assay

To assess the production of OPG by BMSCs, the supernatant was collected and assayed in triplicate for determining OPG concentration via an enzyme-linked immunosorbent assay (ELISA) kit (R&D Systems Inc., Minneapolis, MN, USA). We triplicated the experiment at once, and we carried out this 3 times.

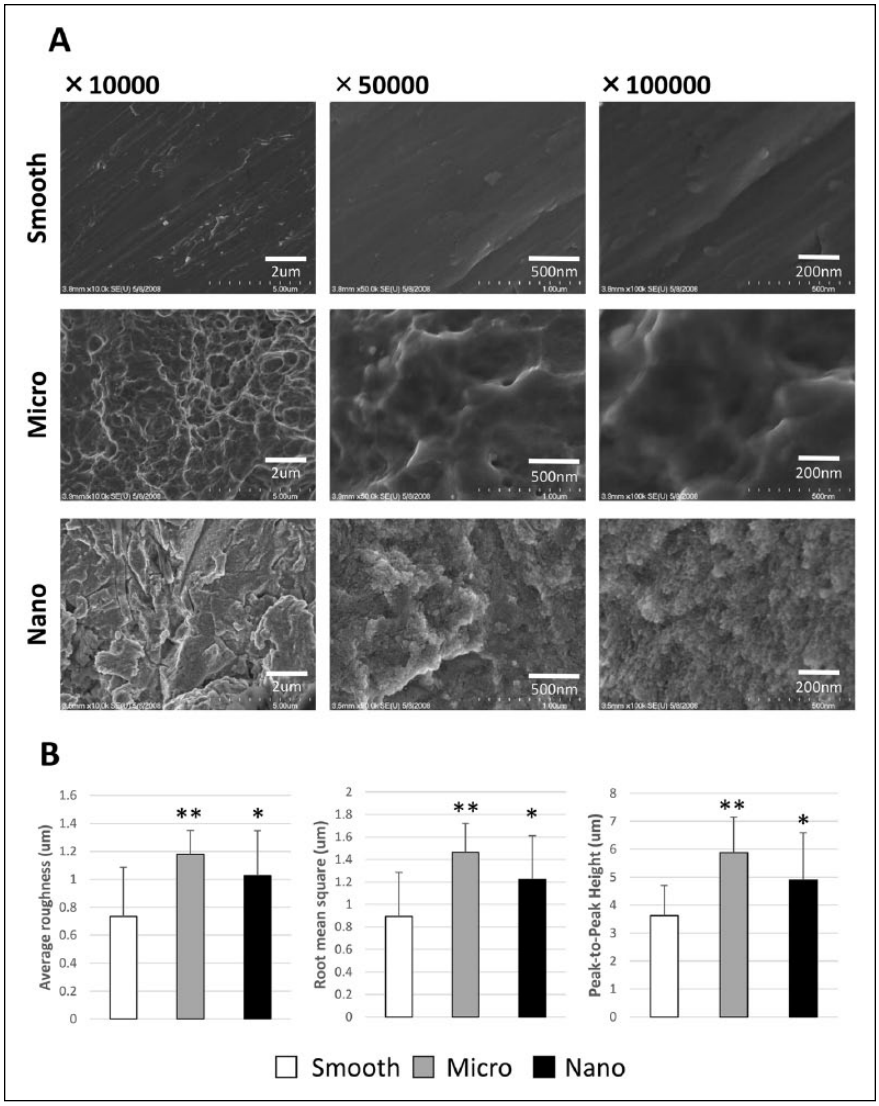

Figure 1. Titanium disks and surface analysis. (**A**) Analysis of the 3 groups (smooth, rough, nano) was performed with high-resolution scanning electron microscopy. (**B**) Atomic force microscopy was performed for average roughness, root mean square, and peak-to-peak height. Observation were made at 3 points on the disk surfaces, and average values and SD were calculated. *$P < 0.05$. **$P < 0.01$.

Statistical Analysis

Statistical analysis was performed with JMP 11 (SAS Institute Inc., Cary, NC, USA). All data were evaluated via analysis of variance, followed by Tukey test. The t test was performed for the comparison of mRNA levels and ELISA results in the 3 topography groups with those of TCP surfaces. Spearman's rank-order correlation was performed to compare the values of BMSC gene expression and osteoclast number on each day. For all statistical analysis, the significance level was set at $P < 0.05$, $P < 0.01$, or $P < 0.001$.

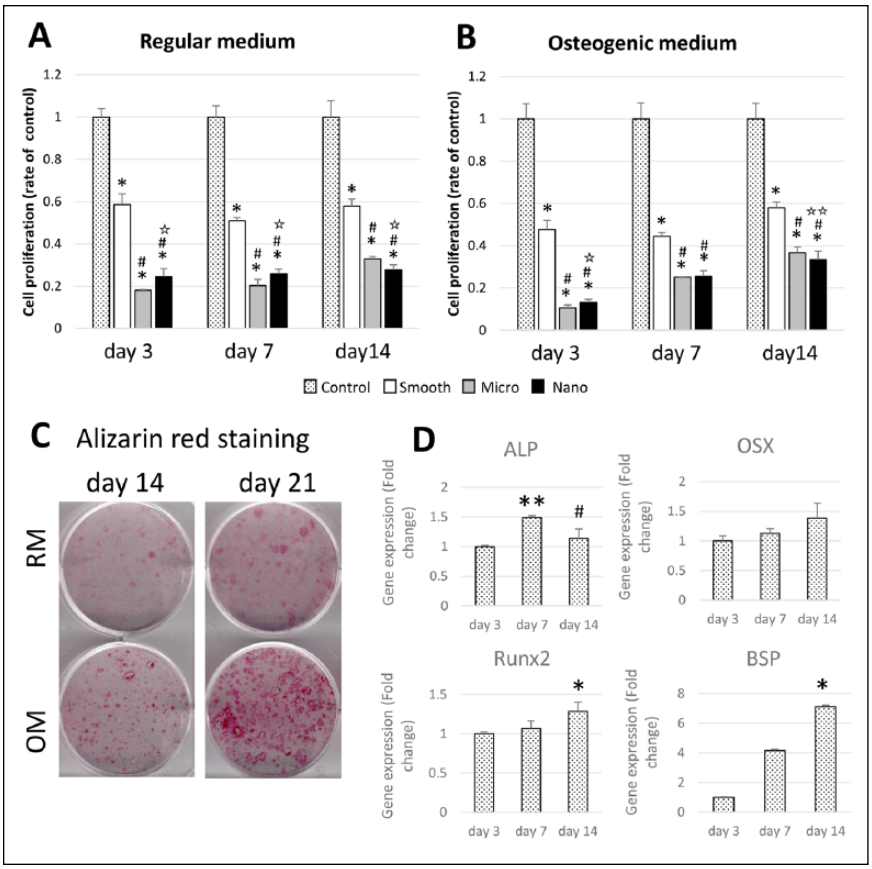

Figure 2. Proliferation, differentiation, and mineralization of bone marrow stromal cells. At 3, 7, and 14 d of bone marrow stromal cell (BMSC) culture on titanium disks (each sample, $n = 6$), the cells were treated with MTS solution in (**A**) regular medium (RM) and (**B**) osteogenic medium (OM) or cell quantification. *$P < 0.001$. #$P < 0.001$. ☆$P < 0.001$, ☆☆$P < 0.05$. (**C**) BMSCs were stained with 2% alizarin red after 14 and 21 d of culture on tissue culture plastic. (**D**) mRNA levels of runt-related transcription factor 2 (Runx2), bone sialoprotein (BSP), osterix (OSX), and alkaline phosphatase (ALP) in BMSCs on tissue culture plastic were analyzed. Relative mRNA abundance was determined by the comparative Ct method and reported as fold induction. GAPDH abundance was used for normalization. *$P < 0.05$. **$P < 0.01$.

Results

Surface Analysis

At low resolution (×10,000), SEM revealed the conservation of M-scale features on M and N surfaces but not on the S surface. At high resolution (×100,000), the presence of discrete 10- to 20-nm N-scale features were observed in the N surface. Few or no N-scale features were observed on the M and S surfaces (Fig. 1A). Atomic force microscopy analysis of surface roughness (average roughness, root mean square, and peak-to-peak height) of the M and N surfaces showed higher scores than those of the S surfaces (**$P < 0.01$, *$P < 0.05$). No significant differences in surface roughness were found between M and N surfaces (Fig. 1B). X-ray photoelectron spectroscopy analysis demonstrated traces of different chemical components on each surface. There was no significant difference in elemental oxygen, carbon, titanium, sodium, nitrogen, and sulfur among S, M, and N surfaces (Table).

Cell Proliferation

The number of BMSCs cultured in RM on S titanium disks was half of that of TCP (control; *$P < 0.001$), and the proliferation rate of BMSCs on M and N disks was further reduced throughout the experimental period (#$P < 0.001$). M surface–adherent cell proliferation was lower than that of cells adherent to the N surface at 3 and 7 d (☆$P < 0.001$) and higher than that of cells adherent to N surface at 14 d (☆$P < 0.001$, ☆☆$P < 0.05$; Fig. 2A, B).

Osteogenic Differentiation

Osteogenic differentiation of BMSCs was induced by culture in osteogenic media as demonstrated by alizarin red staining of cell layer calcification at 14 and 21 d (Fig. 2C). Osteogenesis-related gene expression by BMSCs cultured with OM were analyzed at 3, 7, and 14 d (Fig. 2D). The mRNA levels of ALP were raised at 7 d compared with 3 d (**$P < 0.01$), and the levels of OSX, Runx2, and BSP mRNA expression were increased throughout the experimental period. At day 14, Runx2 and BSP levels were higher than those at 3 d (*$P < 0.05$).

Osteoclast Number and BMM Gene Expression

Osteoclast number (TRAP-positive cells with ≥3 nuclei) was increased among BMMs on addition of BMSC CM (**$P < 0.01$). There was a significant difference between CM(–) and 1:50 and 1:5 dilutions of added CM (Fig. 3A). To ascertain if osteoclast induction was caused by a heat-labile protein in the CM, BMMs were also cultured in the presence of added heat-inactivated CM (50 °C for 2 h). Heat inactivation diminished the effect of BMSC CM in promoting osteoclastogenesis (#$P < 0.05$; Fig. 3B). The influence of surface topography on BMSC contribution to pro-osteoclastogenic factors in CM was notable (Fig. 3C); greater numbers of osteoclasts formed in the presence of CM from BMSCs adherent to M- versus S- or N-scale surfaces. The influence of added CM was BMSC differentiation dependent; CM collected after 7 d of BMSC culture showed the highest osteoclast numbers (##$P < 0.01$; Fig. 3D, E). In animal experiments, implantation of M-scale surface implants resulted in higher osteoclast numbers from tibia-derived BMMs (compared with S [*$P < 0.05$] and N [**$P < 0.01$]; Fig. 3F). Gene expression of BMMs with CM from

BMSCs cultured with RM showed the same tendency as osteoclast number (Fig. 3G, H).

Adherent BMSC Osteoclast-modulating Gene Expression

Gene expression of OPG, TNF-α, and M-CSF is presented in Figure 4A and B. OPG mRNA levels were generally decreased with increasing surface roughness (S > M > N). TNF-α mRNA levels were higher in cells adherent to the M-scale surfaces than others, particularly at day 14. M-CSF mRNA levels were higher in cells adherent to the M- and N-scale surfaces. In consideration of the influence of BMSC differentiation, TNF-α levels were significantly different only at 14 d for the S- and N-scale surface-adherent cells, suggesting that multiple environmental cues (surface, cytokines, and hormones, among others) influence osteoprogenitor cell function. BMSCs grown in OM produced less OPG and greater M-CSF at later time points, further indicating the influence of BMSC differentiation on the expression of factors that modulate BMM osteoclastogenesis.

ELISA

OPG protein expression was modestly increased over the experimental time course. OPG concentration in BMSC culture supernatant was highest for M-adherent cells throughout the period. The temporal pattern of OPG expression in cells adherent to S surfaces differed from other groups (Fig. 4C).

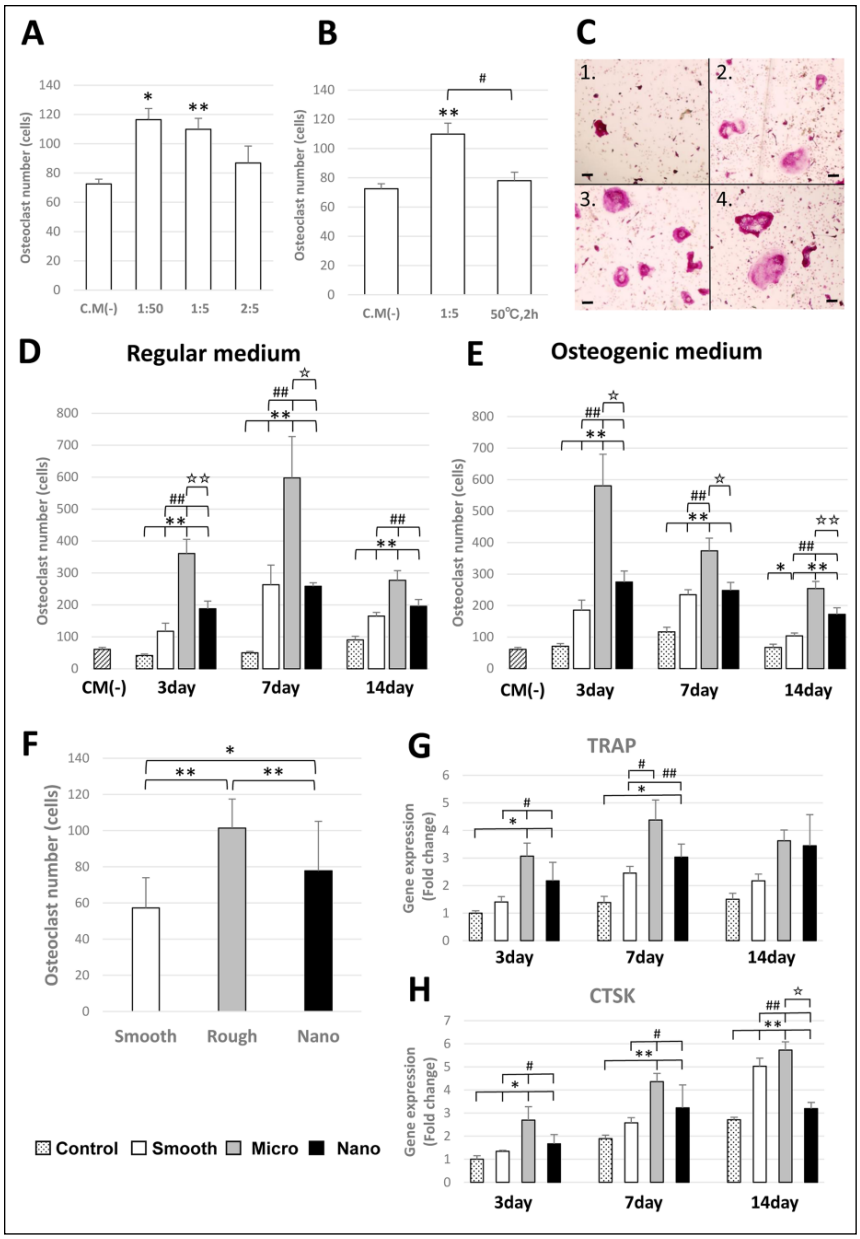

Figure 3. Osteoclast formation assay and bone marrow–derived macrophage gene expression. Tartrate-resistant acid phosphatase (TRAP)–positive cells with ≥3 nuclei were scored as osteoclasts by microscopic counts. All experiments were performed in triplicate (n = 7) for each condition. (**A**) Influence of different ratios of added conditioned media (CM) of bone marrow stromal cells (BMSCs). CM from BMSCs was cultured with regular medium (RM) for 1 d on smooth titanium plate. (**B**) The influence of heat-inactivated CM on osteoclast number. CM from BMSC was cultured with RM for 1 d on smooth titanium plate. (**C**) Osteoclast cultured with CM(–) (C_1) and with M(+) from BMSCs cultured on microsurface for day 3 (C_2), day 7 (C_3), and day 14 (C_4). Bar = 50 μm. (**D**, **E**) A 1:5 concentration of CM was used. The influence of surface topography on BMSCs cultured with RM or OM contribution to pro-osteoclastogenic factors in CM. (**F**) Osteoclast number formed from bone marrow isolated from tibia following placement of smooth, micro, and nano surface implants. (**G**, **H**) Gene expression of TRAP and cathepsin K (CTSK) in bone marrow–derived macrophages with CM from BMSCs cultured with RM. *P < 0.05. **P < 0.01. #P < 0.05. ##P < 0.01.

Discussion

Titanium implant surface topography influences cell behavior in many ways (Shibata and Tanimoto 2015), and osseointegration is accelerated by both M-scale topography modifications (Buser et al. 1991; Ogawa and Nishimura 2003) and N-scale topography modifications (Mendonca et al. 2008; Thakral et al. 2014). The majority of studies have focused on osteoinduction and bone formation by adherent osteoprogenitor cell types (Thalji and Cooper 2014). To date, the importance of bone resorption in the process of bone accrual at implant surfaces has not been explored in detail.

This study demonstrated that BMSCs from rat bone marrow express known osteoclastogenesis-modulating proteins, including OPG, TNF-α, and M-CSF in a titanium surface topography–specific manner. In addition, these cells express

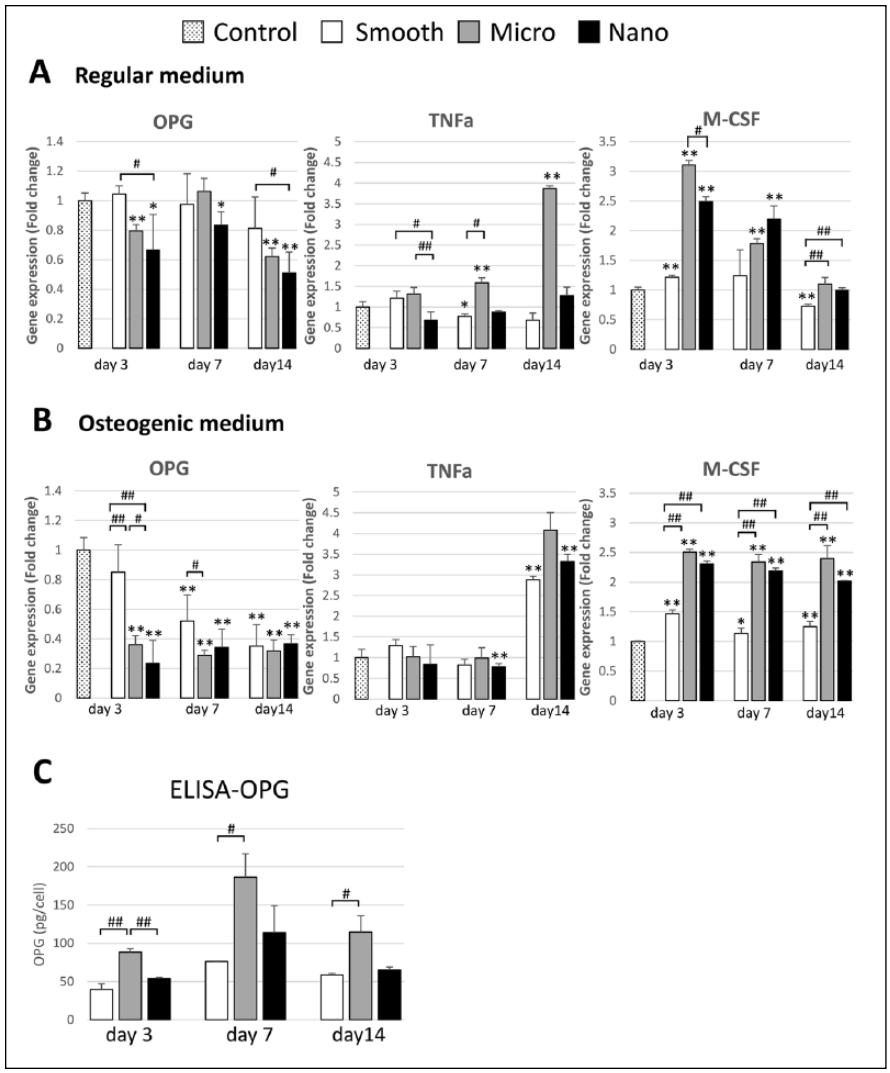

Figure 4. Adherent bone marrow stromal cell (BMSC) osteoclast-modulating gene expression and enzyme-linked immunosorbent assay. Gene expression of osteoprotegerin (OPG), tumor necrosis factor α (TNF-α), and macrophage colony-stimulating factor (M-CSF) in BMSCs cultured with (**A**) regular medium or (**B**) osteogenic medium. (**C**) To assess the production of OPG by BMSCs at each time point (3, 7, 14 d), the supernatant was collected and assayed in triplicate for OPG concentration with enzyme-linked immunosorbent assay (ELISA). $^{*}P < 0.05$. $^{**}P < 0.01$. $^{\#}P < 0.05$. $^{\#\#}P < 0.01$.

the cell surface–bound protein RANKL (data not shown). Furthermore, BMSC-derived proteins influenced BMM-derived osteoclast differentiation. CM from surface-adherent BMSCs increased the number of osteoclasts cultured from rat BMMs in a surface topography–dependent manner and confirmed the presence of putative responsible proteins as heat-labile components of the CM (Fig. 3B).

CM contains various cytokines acting as trophic mediators that regulate neighboring cells (Nakano et al. 2010; Kupcova Skalnikova 2013). Here, the expression of prominent osteoclast-promoting factors TNF-α and M-CSF was increased by BMSCs cultured on both M- and N-scale titanium topographies, independent of exposure to OM (Fig. 4B).

TNF-α stimulates osteoclastogenesis by directly targeting osteoclast progenitors and also influencing osteoclastogenesis indirectly through the stimulation of RANKL and M-CSF expression of stromal cells (Kitaura et al. 2013; Souza and Lerner 2013). Previous reports demonstrated that surface topography contributes to osteoprogenitor cell TNF-α production (Palmquist et al. 2013). Here, the correlation of TNF-α expression with osteoclast number at 7 and 14 d was 0.9993 ($P < 0.01$) and 0.9236, respectively.

M-CSF is produced by stromal cells in bone marrow, osteoblasts, fibroblasts, and lymphocytes. M-CSF enhances osteoclastogenesis (Souza and Lerner 2013). The peak levels of M-CSF mRNA for BMSCs adherent to M-scale surfaces preceded the highest number of osteoclasts observed at day 7. The relationship between BMSC-derived M-CSF and CM-induced osteoclast number is supported by the correlation of M-CSF expression with osteoclast number at 3, 7, and 14 d (0.911 [$P < 0.01$], 0.4449, and 0.7382, respectively). These correlations of M-CSF (day 3) and TNF-α (day 7) with osteoclast number suggest a surface topography–dependent functional relationship that merits further investigation in vivo.

It is widely accepted that OPG is a potent inhibitor of osteoclastogenesis, and previous studies demonstrated that CM from human mesenchymal stem cells inhibits osteoclastogenesis through OPG production (Oshita et al. 2011). OPG expression is elevated on topographically enhanced surfaces (Lossdorfer et al. 2004; Zhao et al. 2007; Schwartz et al. 2009; Galli et al. 2013). Yet, Passeri et al. (2010) reported no influence of surface topography on OPG expression. Here, OPG mRNA protein levels in cultured cells were increased on M-scale surfaces (Fig. 4C). While increasing OPG levels would predict that CM would reduce osteoclastogenesis, an opposite increase in osteoclast number was recorded. In the context of the present experimental model, other factors in CM may influence osteoclastogenesis. The characteristics and subpopulations of osteoclast precursors along with the interaction of osteoclast precursors with cytokines (Asagiri and Takayanagi 2007; Matsubara et al. 2012) should be further explored. As indicated above, M-CSF and TNF-α mRNA levels were significantly increased over time in M- and N-scale-adherent BMSCs.

Osteoclastogenesis may play an important role in the process of osseointegration in at least 2 ways. In the formative stages following implant placement, osteoclast-mediated removal of necrotic bone at the interface is necessary and has

been demonstrated in human histologic investigations (Bosshardt et al. 2011). The rapid rate of woven bone formation on moderately rough dental implants that is attributed to surface topography must be followed by functional bone remodeling in a time frame relevant to implant function (Shalabi et al. 2006). Thus, induction of osteoclast function during the formative phase of osseointegration is necessary, and transiently increased numbers of osteoclasts may not be contrary to the overall accrual of bone mass by an integrated regulation of bone formation and resorption. The influence of osteoclasts on bone accrual at the bone-to-implant interface has been clearly demonstrated by adiponectin-mediated suppression of osteoclastogenesis that increased bone-to-implant contact in the ovariectomized rabbit tibia model (Luo et al. 2012). This cell culture model demonstrated expression and directed modulation of several key factors that influence osteoclastogenesis in vivo. The present in vivo data showed that osteoclastogenesis was highest when signaling from BM of M-scale surface–implanted tibia was used (Fig. 3F). Regarding the ongoing process of remodeling that preserves the osseointegrated bone-to-implant interface, the present cell culture model may not represent the biomechanical and biological spectrum of factors that control this process. However, signaling from cells adherent to the implant surface represent one of many local cues relevant to peri-implant cellular function.

In conclusion, this study revealed that surface topography–specific alterations in BMSC function influenced cell culture–mediated BMM-derived osteoclastogenesis and demonstrated that surface topography influences local cells in vivo. To comprehensively understand the complex biological events occurring in the bone-implant interface, detailed studies of osteoclastogenesis should be performed in the context of implant topography.

Author Contributions

M. Nagasawa, contributed to conception, design, data acquisition, analysis, and interpretation, drafted and critically revised the manuscript; L.F. Cooper, K. Uoshima, contributed to conception, design, and data interpretation, drafted and critically revised the manuscript; Y. Ogino, contributed to conception, data acquisition, analysis, and interpretation, critically revised the manuscript; D. Mendonca, contributed to data analysis and interpretation, critically revised the manuscript; R. Liang, S. Yang, G. Mendonca, contributed to data acquisition, critically revised the manuscript. All authors gave final approval and agree to be accountable for all aspects of the work.

Acknowledgments

This work was financially supported by UNC DENTSPLY PDPA. The authors thank Dr. Yujin Aoyagi for his assistance with the titanium surface analysis. The authors declare no potential conflicts of interest with respect to the authorship and/or publication of this article.

References

Asagiri M, Takayanagi H. 2007. The molecular understanding of osteoclast differentiation. Bone. 40(2):251–264.

Bosshardt DD, Salvi GE, Huynh-Ba G, Ivanovski S, Donos N, Lang NP. 2011. The role of bone debris in early healing adjacent to hydrophilic and hydrophobic implant surfaces in man. Clin Oral Implants Res. 22(4):357–364.

Buser D, Schenk RK, Steinemann S, Fiorellini JP, Fox CH, Stich H. 1991. Influence of surface characteristics on bone integration of titanium implants: a histomorphometric study in miniature pigs. J Biomed Mater Res. 25(7):889–902.

Dalby MJ, Gadegaard N, Curtis AS, Oreffo RO. 2007. Nanotopographical control of human osteoprogenitor differentiation. Curr Stem Cell Res Ther. 2(2):129–138.

Fujii N, Kusakari H, Maeda T. 1998. A histological study on tissue responses to titanium implantation in rat maxilla: the process of epithelial regeneration and bone reaction. J Periodontol. 69(4):485–495.

Futami T, Fujii N, Ohnishi H, Taguchi N, Kusakari H, Ohshima H, Maeda T. 2000. Tissue response to titanium implants in the rat maxilla: ultrastructural and histochemical observations of the bone-titanium interface. J Periodontol. 71(2):287–298.

Galli C, Piemontese M, Lumetti S, Manfredi E, Macaluso GM, Passeri G. 2013. GSK3b-inhibitor lithium chloride enhances activation of Wnt canonical signaling and osteoblast differentiation on hydrophilic titanium surfaces. Clin Oral Implants Res. 24(8):921–927.

Kang H, Chang W, Hurley M, Vignery A, Wu D. 2010. Important roles of PI3Kgamma in osteoclastogenesis and bone homeostasis. Proc Natl Acad Sci U S A. 107(29):12901–12906.

Kitaura H, Kimura K, Ishida M, Kohara H, Yoshimatsu M, Takano-Yamamoto T. 2013. Immunological reaction in TNF-alpha-mediated osteoclast formation and bone resorption in vitro and in vivo. Clin Dev Immunol. 2013:181849.

Klokkevold PR, Han TJ. 2007. How do smoking, diabetes, and periodontitis affect outcomes of implant treatment? Int J Oral Maxillofac Implants. 22 (Suppl):173–202.

Kupcova Skalnikova H. 2013. Proteomic techniques for characterisation of mesenchymal stem cell secretome. Biochimie. 95(12):2196–2211.

Lossdorfer S, Schwartz Z, Wang L, Lohmann CH, Turner JD, Wieland M, Cochran DL, Boyan BD. 2004. Microrough implant surface topographies increase osteogenesis by reducing osteoclast formation and activity. J Biomed Mater Res A. 70(3):361–369.

Luo E, Hu J, Bao C, Li Y, Tu Q, Murray D, Chen J. 2012. Sustained release of adiponectin improves osteogenesis around hydroxyapatite implants by suppressing osteoclast activity in ovariectomized rabbits. Acta Biomater. 8(2):734–743.

Masuda T, Salvi GE, Offenbacher S, Felton DA, Cooper LF. 1997. Cell and matrix reactions at titanium implants in surgically prepared rat tibiae. Int J Oral Maxillofac Implants. 12(4):472–485.

Matsubara R, Kukita T, Ichigi Y, Takigawa I, Qu PF, Funakubo N, Miyamoto H, Nonaka K, Kukita A. 2012. Characterization and identification of subpopulations of mononuclear preosteoclasts induced by TNF-α in combination with TGF-β in rats. PLoS One. 7(10):e47930.

Mendonca G, Mendonca DB, Aragão FJ, Cooper LF. 2008. Advancing dental implant surface technology: from micron- to nanotopography. Biomaterials. 29(28):3822–3835.

Mendonca G, Mendonca DB, Aragão FJ, Cooper LF. 2010. The combination of micron and nanotopography by H(2)SO(4)/H(2)O(2) treatment and its effects on osteoblast-specific gene expression of hMSCs. J Biomed Mater Res A. 94(1):169–179.

Minkin C, Marinho VC. 1999. Role of the osteoclast at the bone-implant interface. Adv Dent Res. 13:49–56.

Nakano N, Nakai Y, Seo TB, Yamada Y, Ohno T, Yamanaka A, Nagai Y, Fukushima M, Suzuki Y, Nakatani T, et al. 2010. Characterization of conditioned medium of cultured bone marrow stromal cells. Neurosci Lett. 483(1):57–61.

Ogawa T, Nishimura I. 2003. Different bone integration profiles of turned and acid-etched implants associated with modulated expression of extracellular matrix genes. Int J Oral Maxillofac Implants. 18(2):200–210.

Ogino Y, Liang R, Mendonça DB, Mendonça G, Nagasawa M, Koyano K, Cooper LF. 2016. RhoA-mediated functions in C3H10T1/2 osteoprogenitors are substrate topography-dependent. J Cell Physiol. 231(3):568–575.

Ogle OE. 2015. Implant surface material, design, and osseointegration. Dent Clin North Am. 59(2):505–520.

Oshita K, Yamaoka K, Udagawa N, Fukuyo S, Sonomoto K, Maeshima K, Kurihara R, Nakano K, Saito K, Okada Y, et al. 2011. Human mesenchymal stem cells inhibit osteoclastogenesis through osteoprotegerin production. Arthritis Rheum. 63(6):1658–1667.

Palmquist A, Johansson A, Suska F, Brånemark R, Thomsen P. 2013. Acute inflammatory response to laser-induced micro- and nano-sized titanium surface features. Clin Implant Dent Relat Res. 15(1):96–104.

Passeri G, Cacchioli A, Ravanetti F, Galli C, Elezi E, Macaluso GM. 2010. Adhesion pattern and growth of primary human osteoblastic cells on five commercially available titanium surfaces. Clin Oral Implants Res. 21(7):756–765.

Schwartz Z, Olivares-Navarrete R, Wieland M, Cochran DL, Boyan BD. 2009. Mechanisms regulating increased production of osteoprotegerin by osteoblasts cultured on microstructured titanium surfaces. Biomaterials. 30(20):3390–3396.

Shalabi MM, Gortemaker A, Van't Hof MA, Jansen JA, Creugers NH. 2006. Implant surface roughness and bone healing: a systematic review. J Dent Res. 85(6):496–500. Erratum in: J Dent Res. 2006;85(7):670.

Shibata Y, Tanimoto Y. 2015. A review of improved fixation methods for dental implants: part I. Surface optimization for rapid osseointegration. J Prosthodont Res. 59(1):20–33.

Souza PP, Lerner UH. 2013. The role of cytokines in inflammatory bone loss. Immunol Invest. 42(7):555–622.

Takayanagi H, Ogasawara K, Hida S, Chiba T, Murata S, Sato K, Takaoka A, Yokochi T, Oda H, Tanaka K, et al. 2000. T-cell-mediated regulation of osteoclastogenesis by signalling cross-talk between RANKL and IFN-gamma. Nature. 408(6812):600–605.

Thakral G, Thakral R, Sharma N, Seth J, Vashisht P. 2014. Nanosurface: the future of implants. J Clin Diagn Res. 8(5):ZE07–ZE10.

Thalji G, Cooper LF. 2013. Molecular assessment of osseointegration in vivo: a review of the current literature. Int J Oral Maxillofac Implants. 28(6):e521–e534.

Thalji G, Cooper LF. 2014. Molecular assessment of osseointegration in vitro: a review of current literature. Int J Oral Maxillofac Implants. 29(2):e171–e199.

Zhao G, Raines AL, Wieland M, Schwartz Z, Boyan BD. 2007. Requirement for both micron- and submicron scale structure for synergistic responses of osteoblasts to substrate surface energy and topography. Biomaterials. 28(18):2821–2829.